THESIS FOR THE DEGREE OF LICENTIATE OF ENGINEERING

Interactions Between Water and Cellulose Esters

The effect of the acyl side-chain length

ROBIN NILSSON

Department of Chemistry and Chemical Engineering

CHALMERS UNIVERSITY OF TECHNOLOGY

Gothenburg, Sweden 2022

Interactions Between Water and Cellulose Esters
The effect of the acyl side-chain length
ROBIN NILSSON

© ROBIN NILSSON, 2022.

Technical report no 2022:05

Department of Chemistry and Chemical Engineering
Chalmers University of Technology
SE-412 96 Gothenburg
Sweden
Telephone + 46 (0)31-772 1000

Cover: Photography illustrating films exposed to droplets of water. The cross-section of a spruce underneath and surrounding branches represents the renewable resources the materials can be made from. Photo taken by Robin Nilsson.

Printed by Chalmers Reproservice
Gothenburg, Sweden 2022

Interactions Between Water and Cellulose Esters

The effect of the acyl side-chain length

ROBIN NILSSON

Department of Chemistry and Chemical Engineering

Chalmers University of Technology

Abstract

Biopolymers, which are produced from natural sources, are gaining interest as a potential replacement for fossil-based polymers. As such, they are already widely used in several industries, including the food, healthcare, and personal care industries. To harness the full potential of biopolymers as materials in new products designed for specific tasks, an ability to accurately predict their properties and how these properties change in different environments, is desirable. Hansen Solubility Parameters (HSP) combine dispersive, polar, and hydrogen bonding energies to understand interactions between molecules. This thesis explores the potential use of HSP as predictors of glass transition temperatures (T_g) and water interactions. It also focuses on elucidating the effect of an increased side-chain length of cellulose esters on their thermal properties, structural properties, and water interactions, together with how these properties are affected by the absorption of water. The cellulose esters studied here were cellulose acetate, cellulose acetate propionate, and cellulose acetate butyrate.

The HSP showed that the dispersive energy dominates the total cohesive energy, followed by the hydrogen bonding and then the polar energy. Counter-intuitively, the T_g decreased with an increased total cohesive energy. The HSP explained this phenomenon, namely, that the increased length of the substituents screened the short-range hydrogen bonds. A similar effect was observed for water solubility and penetration into the cellulose esters, which decreased with increasing side-chain lengths despite the approximately constant hydrogen bonding energies. This indicates the importance of focusing on each of the different interaction parameters instead of only the total HSP.

***Keywords**: cellulose acetate, glass transition, water absorption, water diffusion, Hansen Solubility Parameters, wide-angle X-ray scattering*

“Who knows? Have patience. Go where you must go, and hope!” - Gandalf

List of Publications

This thesis is based on the following appended papers:

I. **Screening of hydrogen bonds in modified cellulose acetates with alkyl chain substitutions**, Robin Nilsson, Martina Olsson, Gunnar Westman, Aleksandar Matic and Anette Larsson
Carbohydrate Polymers, vol. 285, 2022, 119188, DOI:10.1016/j.carbpol.2022.119188.

II. **Experimental and simulated distribution and interaction of water in cellulose acetates with alkyl chain substitution**, Robin Nilsson, Hüsamettin Deniz Özeren, Okky Putra, Mikael Hedenqvist, Anette Larsson
Submitted

Contribution Report

My authorship contributions to this thesis are as follows:

I. Main author. Planned and performed the experimental work, except for the wide-angle X-ray scattering (WAXS) experiments, which were performed by Martina Olsson. Analyzed and interpreted the results in collaboration with the co-authors. Wrote the original draft of the manuscript and reviewed and edited the article with support from Anette Larsson and the other co-authors.

II. Main author. Planned the experimental work and wrote the original draft. Hüsamettin Deniz Özeren performed the molecular dynamics simulations and helped interpret the data. Okky Putra performed the dynamic vapor sorption measurements. Analyzed and interpreted the results in collaboration with the co-authors. Revision and editing were done with support from the co-authors.

Abbreviations

AGU	1,4-anhydro-D-glucose units
CA	Cellulose acetate
CAB	Cellulose acetate butyrate
CAP	Cellulose acetate propionate
DS	Degree of substitution
DSC	Differential scanning calorimetry
DVS	Dynamic vapor sorption
EC	Ethyl cellulose
FTIR	Fourier transform infrared spectroscopy
HSP	Hansen Solubility Parameters
MD	Molecular dynamics
NMR	Nuclear magnetic resonance
OH	Hydroxyl group
DOH	Degree of hydroxyl groups
PP	Polypropylene
RH	Relative humidity
TGA	Thermogravimetric analyzer
WAXS	Wide-angle X-ray scattering

Symbols

$C_a(t)$	Concentration on the acceptor side at time t
$C_{d,0}$	Concentration on the donor side at time 0
DS_A	Degree of substitution of acetyl
DS_B	Degree of substitution of butyryl
DS_P	Degree of substitution of propionyl
DS_{tot}	Total degree of substitution
E_d	Dispersive cohesive energy
E_h	Hydrogen bonding energy
E_p	Polar cohesive energy
E_{tot}	Total cohesive energy
h	Thickness
M_n	Average molecular weight
t	Time
T_2O	Tritium water
T_d	Degradation temperature
T_g	Glass transition temperature
T_m	Melting temperature
V	Volume of acceptor chamber
V_{molar}	Molar volume
ΔH_f	Enthalpy of fusion
δ_d	Dispersive parameter
δ_h	Hydrogen bonding parameter
δ_p	Polar parameter
δ_{tot}	Total Hansen Solubility Parameter

Contents

1 | Introduction

One of the main trends in modern development is the transition from fossil-based resources to renewable, bio-based alternatives, thereby reducing pollution and contributing towards achieving a circular economy. In 2019, European plastic production amounted to 50.7 million tons, of which up to 39.6% consisted of packaging. Plastics have historically been produced from fossil fuels; however, the non-renewable nature of fossil-based resources means that they cannot be relied upon to continue to supply a large and increasing demand. Consequently, plastics that are based on renewable and recyclable resources are needed [1].

Polymers made from natural sources such as trees are called biopolymers. Cellulose is an example of a biopolymer and is one of few that are available in large enough quantities to be a viable candidate for substituting fossil-based polymers in industries like the plastics packaging industry. Since cellulose can be extracted from trees, it has become a biopolymer of interest in countries like Sweden, where the productive forest area is large (22.5 million hectares in 2011) [2]. However, one notable drawback with biopolymers like cellulose is that their properties may change in response to humidity and water, making their suitability questionable for applications where humidity varies or where direct contact with water may occur. This is a challenge for films in food packages where they need to have structural integrity and be impenetrable to gases, independent of moisture present either inside the package or arising from the external environment. Another drawback with cellulose is its low melt processability relative to polymers usually encountered in plastics. To address both the aforementioned challenges, chemical modification of cellulose may be a solution. It is commonly conducted by adding side-chains to the cellulose backbone to form cellulose derivatives. A large variety of cellulose derivatives exist on the market, including cellulose ethers (methyl cellulose, ethyl cellulose (EC), hydroxypropyl cellulose, hydroxypropyl methyl cellulose) and cellulose esters (cellulose acetate (CA), cellulose acetate propionate (CAP), cellulose acetate butyrate (CAB), and cellulose acetate phthalate (CAP)). Cellulose derivatives are used in many areas such as pharmaceutics, cosmetics, food, and construction, where they often serve as the critical component. EC and CA are two examples of cellulose derivatives used in applications with large water resistance. EC is used in thin-film coatings for pharmaceutics, in paper, and as a water-insoluble food thickener. CA is commonly used in membrane applications, *e.g.*, in water retention and salt separation.

In literature, water interactions with biopolymers have been associated with their hydroxyl groups (-OH). It is generally accepted that the major contributor to the water sensitivity of cellulose derivatives is the formation of strong hydrogen bonds within the structure. Here, water will orient towards hydrophilic groups, such as hydroxyl groups, in cellulose via hydrogen bonding [3]. These strong molecular interactions are the reason why materials with many hydroxyl groups absorb large amounts of water. This thesis focuses instead on the effect of the length of substituents´ side-chains on interactions with water. Therefore, cellulose esters with a similar degree of hydroxyl groups were investigated.

Tools that allow the prediction of materials' behaviours based solely on their molecular structure are desirable. An example of such a predictive tool is the Hansen Solubility Parameters (HSP), which are mainly used to predict solubilities of polymers in solvents but have also been used for other purposes, such as predicting the dispersibility of crystalline nanocellulose in low-density polyethylene [4] or explaining the variation in resin swelling in binary solvents [5]. A study closely related to this work is one by Ramanaiah et al., where temperature-induced changes in experimentally determined HSP were studied for CAP and CAB [6], [7]. Another closely related study by Ong et al. focused on salt retention in CAP and CAB and how this could be related to HSP [8].

1.1 Aim and Objective

This thesis aims to provide insights into how small changes in the chemical structure of cellulose derivatives may alter their properties, how they interact with water, and how water affects their properties. As specific examples of cellulose derivatives, this thesis is limited in scope to CA, CAP, three types of CAB comprising different degrees of substitution of butyrate (denoted CABI, CABII, and CABIII), and EC. This limited scope should be considered in the interpretation and generalizability of the results. The following objectives are put in focus:

1) To characterize and produce hot-melt pressed films of the selected set of cellulose derivatives.
2) To investigate how water interacts with these cellulose derivatives during full submersion in water and upon exposure to different relative humidities (RH).
3) To characterize how absorbed water affects the density and microstructure of the materials.
4) To investigate the correlation between calculated HSP and thermal properties and water interactions of all materials.

The content of this thesis is based on two studies, the appended Papers I and II. Paper I focuses on how the side-chain length of CA, CAP, and CABI-III affects their thermal and structural properties, water absorption, and water diffusion. Additionally, it investigates if the HSP of the materials can be correlated to their glass transition temperatures, water absorption, and water diffusion. Paper II uses the same materials but focuses instead on how the side-chain length affects the position where water is absorbed in the structure. This was investigated by studying absorption isotherms for the materials over a wide range of RH (0-80% RH) and by molecular dynamics (MD) simulations. The MD simulations were performed in collaboration with Hüsamettin Deniz Özeren and Mikael Hedenqvist and will not be covered in great detail in this thesis.

1.2 FibRe VINNOVA Competence Center

This work was performed in association with FibRe in August 2021. FibRe is a VINNOVA competence center, which operates as a research consortium involving Chalmers University of Technology, KTH Royal Institute of Technology, industry, and public organization partners. One of FibRe´s short-term goal is "to understand how thermoplasticity for lignocellulose-based materials depends on the molecular structure." The present project focuses specifically on this goal and, by extension, to FibRe.

2 | Cellulose and Cellulose Ester

Cellulose is a linear homopolymer of 1,4-anhydro-D-glucose units (AGU) linked by β-1,4 glycosidic linkages between carbons C_1 and C_4, Figure 1a. The repeating unit of cellulose consists of two AGUs, which are rotated 180°C with respect to each other [9,10]. Figure 1b shows the cellulose base, where the hydroxyl hydrogens have been exchanged for other groups. The number of substitutions per unit is commonly referred to as the degree of substitution (DS). Examples of substituents (and the resulting cellulose derivatives) are acetyl (CA), a mixture of acetyl and propionyl (CAP), a mixture of acetyl and butyryl (CAB), and ethyl (EC).

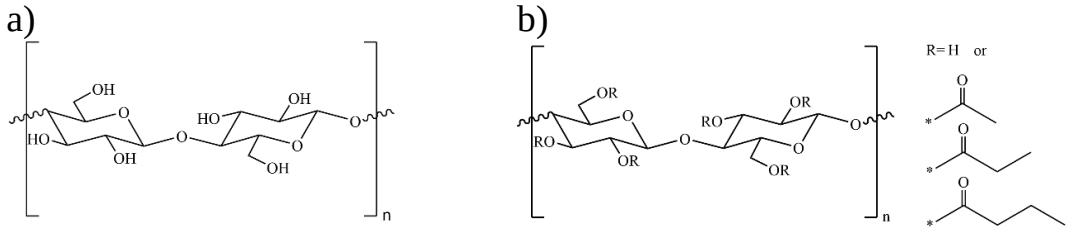

Figure 1. The chemical structure of a) cellulose and b) cellulose where R is either a hydroxyl, acetyl, propionyl, or butyrate group.

The first mention of cellulose acetate was in the late 19th century when it was discovered that it could be produced by mixing cellulose and acetic anhydrate. Transitioning into the 20th century, patents for photographic film and artificial silk appeared, but the market was cold due to specially cleaned cotton being needed as a raw material and new processing methods being needed for the synthesis. Instead, another CA with lower degree of substitution, cellulose diacetate, achieved interest due to its solubility in common solvents such as acetone and chloroform [11]. This facilitated its application in airplane coatings, replacing heavier rubber whilst being more resistant to water, oil, and petroleum [12]. The growing demand in the aircraft industry during World War I drove industrial production further and, after the war, the production of cellulose diacetate yarn was initiated with new fiber spinning techniques [13]. The advent of polyester and nylon decreased the production of cellulose diacetate yarn. The next large usability of CA was as filters in cigarettes, where it regained popularity in the 1950s, with high usage continuing to 2014 where it was included in 80% of the world's cigarettes [14]. Cellulose di- and triacetate can also be mixed with plasticizers or mixed with cellulose esters and processed by injection molding into a variety of products like tool handles and toys. The rupture and splicing resistance of CA also made it a preferred material for photographic and motion film as well as security glass for automobiles. By 2016, the global market for CA was 614 kt [14] and, recently, there has been an interest in CA as a coating component in LCD screens [15].

Alternative commercially available cellulose esters to CA are CAP and CAB [16]. They are both easier to dissolve than CA, making them practical for many applications. CAB is used in areas such as binders in decorative and protective coatings in human nail care, leather, paper, plastic, trucks, and buses. In these applications, CAB provides toughness, weather resistance, flexibility, color retention, and more. CAP is similar to CAB and is used where low odor is needed. CAP can for instance be mixed with plasticizers and made into products like toothbrushes [14]. CAP, CAB, and CA have also gained interest in the field of water purification because of their salt retention and water flux characteristics, which are adjustable by controlling the substitution of different side groups [17], [18]. CAB, in particular, has shown to be a promising carrier for pharmaceutical substances due to its high encapsulation efficiency compared to EC [19].

This thesis studied five different cellulose esters, namely CA, CAP, and three CAB with different DS. In addition to the esters, the cellulose ether, EC, was also studied and compared to the esters. All cellulose derivatives were selected to have a similar number of unsubstituted hydroxyl groups since the literature has shown that these hydroxyl groups have a large impact on the cellulose derivatives' properties.

3| Thermal Properties

A key feature of plastics is their thermal properties, which gives them desirable mechanical properties and enables melt processing into desirable shapes. For melt processing, the degradation temperature (T_d) is critical to prevent degradation of the materials during processing and further changes in properties like tensile strength, shape, and color that may occur as a consequence of degradation [14]. Two additional thermal properties of importance are a material's glass transition temperature (T_g) and melting temperature (T_m). The T_g is a defined temperature range over which materials transition from a stiff "glassy" state to a softer "rubbery" state. It can also be explained by a gain in energy during the glassy to rubbery transition, which increases the mobility of polymer chains, both in the backbone and side-chains of polymers, resulting in a drastic increase in material flexibility [20]. This means that for a material with low T_g, less energy is needed to increase polymer mobility. The T_g is related to many structural factors such as segment length of the polymer, symmetry, side-chain mobility, backbone mobility, crystallinity, and the material's thermal and processing history [21].

The structure of an amorphous material has only amorphous regions, which results in the material having a T_g but no T_m, whereas semicrystalline materials, for example, polyethylene (PE) and polypropylene (PP), have both amorphous and crystalline regions resulting in both T_g and T_m [22]. Semicrystalline unmodified cellulose has a T_g around 230-245°C and moderate thermal stability, with its thermal processing being limited by rapid chemical decomposition at temperatures above 250°C [10]. Consequently, producing a plastic material from cellulose requires it to be modified to become thermoplastic and melt-processable. Many modified cellulose derivatives, like CA, CAP, CAB, and EC with large DS values, have both a T_g and a T_m, and therefore melt when exposed to high enough temperatures. For CA, studies have shown that when DS increases, the T_g decreases. For example, a CA with a DS of 1.75 can have a T_g of 214°C, which decreases to 200°C when DS increases to 2.45. A similar relationship between DS and T_m can be seen. Continuing the previous example, a CA with a DS of 1.75 that melts at 245°C, instead melts at 233°C when DS increases to 2.45 [23]. By adding longer side-chains, propionate for CAP and butyrate for CAB, T_g and T_m decrease with increasing DS for the respective side-chain, with butyrate contributing more to this decrease than propionate [24].

4| Water Sensitivity

As previously mentioned, biopolymers are known to be sensitive to water, some more than others. Familiar everyday examples of this include a newspaper left outdoors or a food wastepaper bag that, after contact with water, starts to decompose until it eventually loses enough structural integrity to break. Even for relatively water-resistant biopolymers, water is recognized as having a plasticizing effect [25]. In products like packaging materials, water resistance is essential for keeping the products inside the package dry (or wet). Additionally, the water sensitivity of packaging can affect other desired properties such as gas permeation, where a good gas barrier is desired [26]. Carbohydrates are water-sensitive and it has been observed that an increase in water content results in a decrease in T_g [25]. Even water-resistant polymers like PP absorb some water, however, they have a negligible loss in structural integrity [27]. For hydrophilic polymers like cellulose, water can exist in three different ways when absorbed into the structure. These can be referred to as non-freezing water, which is difficult to observe, freezing bound water, which is less closely associated with the polymer, and free water [28].

The amount of water the structures absorb depends on the outside RH and, therefore, studies on how materials behave at different RH are relevant. A common method to characterize the amount of water absorbed is dynamic vapor sorption (DVS), which studies the water vapor sorption of a material at a constant temperature, *i.e.*, a sorption isotherm. In addition to indicating how water is distributed in a material, the shape of the sorption isotherm is material-specific and therefore serves as a fingerprint. A cellulose surface follows a sigmoidal shape, with initially high sorption into a monolayer, followed by the formation of multilayers at larger RH [29]. A common sorption phenomenon among water-sensitive

materials, like chitosan, starch, and cellulose, is that the desorption and absorption are not the same, resulting in a hysteresis [30], [31], [32]. CA also shows a hysteresis in most cases [33], [34].

An important part of water interactions in packaging is the water transport through fully saturated polymer films or membranes. Many properties affect the rate of transport, such as crystallinity, plasticizers, and the chemical structure of the polymer, which includes the degree of cross-linking, tacticity, and molecular weight. Two models can describe mass transport and permeability in polymers. One model is based on free volume theory, where the diffusion constant is related to the free volume of the polymer and the other model is based on intermolecular forces in combination with the motion of the permeant and the polymer chains [35]. Many models have been used to describe the transport of solvents through membranes. A popular one for dense materials, like the polymer used in this study, is the solution-diffusion model. It is based on four assumptions: a homogenous and non-porous morphology is present, the solvent and solute transport have individual concentration profiles through the membrane, the solute and solvent each have their own chemical potential, and lastly, the chemical gradient is due to concentration and pressure gradients across the films. The permeation through membranes occurs in three steps: The solutes first attach to the surface of the membrane, then they diffuse through the bulk of the membrane, then, upon reaching the other side of the membrane, they leave the membrane. The rate-limiting step is the diffusion through the membrane [36]. Calculating water flows are based on Fick's first law of diffusion, further discussed in Section 6.4.

5 | Hansen Solubility Parameters

As mentioned, these parameters are typically used to find suitable solvents for materials by a "like dissolves like" principle [37]. The total HSP squared (δ_{tot}^2) is defined as the total cohesive energy (E_{tot}) divided by the molar volume (V_{molar}), Equation 1.

$$\delta_{tot}^2 = \frac{E_{tot}}{V_{molar}} = \frac{E_d + E_p + E_h}{V_{molar}} = \delta_d{}^2 + \delta_p{}^2 + \delta_h{}^2 \qquad (1)$$

The total cohesive energy comprises energies emerging from three molecular interactions, namely, dispersive forces, polar forces, and hydrogen bonding forces. The dispersive forces are the most general and emerge from nonpolar interactions between atoms, which exist for all molecules. For molecules with only dispersive forces, like a saturated aliphatic hydrocarbon, the energy of vaporization is the same as the dispersive cohesive energy (E_d). Polar forces, or polar cohesive energies (E_p), arise from permanent dipole-permanent dipole interactions. Hydrogen bonding energy (E_h) is the third type of cohesive energy, which arises from molecular interactions similar to polar interactions but with stronger permanent dipole interactions. In Hansen's approach, E_h is simplified as the resulting energy upon subtracting the dispersive and polar forces from the total cohesive energy. Each of these three energies is represented in HSP theory as a dispersion parameter (δ_d), polar parameter (δ_p), and hydrogen bonding parameter (δ_h). These can be experimentally determined for materials using a series of solvents [38]. In this thesis, the solubility parameters were calculated theoretically via an additive method by van Krevelen, which includes dispersive, polar, and hydrogen bonding components for each chemical group [39]. For further information about how the calculations were performed, see Paper I.

6 | Experimental Procedures

In this section, the materials used, namely CA, CAP, CAB, and EC, are explained regarding their chemical structure. Thereafter, the major experimental methods are described, including film preparation methods, thermal property investigations, water absorption studies, and water diffusion studies. For further details regarding experimental methods like FTIR, NMR, WAXS, and HSP, see Paper I and for density measurements and DVS studies, see Paper II.

6.1 Characterization of Materials

The six materials used are displayed in Table 1, together with each of their number average molecular weights (M_n) and DS. The esters were purchased from Sigma Aldrich, Sweden, and the ether was purchased from Dow Wolff Cellulosics GmbH, Germany. M_n values in the table are quoted from the manufacturers. NMR was used to determine the DS for each cellulose derivative (see Paper I). As mentioned, all the esters have a similar high substitution of acyl groups (the collective name for acetyl, propionyl, and butyryl), with the remaining side groups consisting of hydroxyl groups. For CAP, only a small amount of acetyl groups was present in excess to the propionyl and hydroxyl groups. The three butyrate substituted esters have a low, medium, and high degree of substitution of butyrate, with the remaining substitution consisting of acetyl groups.

Table 1. Molecular weight (M_n), degree of substitution (DS) and HSP for the esters (CA, CAP, and CAB) and the ether (EC).

Material	M_n [kDa][1]	DS_{tot}	DS_A	DS_P/ DS_B[2]	DOH	δ_d $(J\ cm^{-3})^{1/2}$	δ_p $(J\ cm^{-3})^{1/2}$	δ_h $(J\ cm^{-3})^{1/2}$	δ_{tot} $(J\ cm^{-3})^{1/2}$
CA	50	2.41	2.41	-	0.59	19.0	6.2	14.5	24.7
CAP	75	2.85	0.21	2.64	0.15	18.2	4.5	11.3	21.9
CABI	65	2.85	2.14	0.71	0.15	18.4	5.0	11.9	22.4
CABII	30	2.80	1.12	1.68	0.20	18.2	4.3	11.2	21.8
CABIII	30	2.71	0.14	2.57	0.29	18.1	3.9	10.9	21.5
EC	-	2.56	-	-	0.45	18.1	5.2	11.3	22.0

[1] M_n provided by suppliers

[2] DS_P/DS_B mean degree of propionyl and butyryl, respectively

6.2 Film Preparation

There are two main methods of making polymer films, either melt processing or solvent casting. The latter is common in research as many polymers have solvents in which they are soluble. This applies to the majority of studies on CA, CAP, and CAB, where acetone and N-methylpyrrolidone have been used [8], [40], [41]. In this study, hot-melt pressing was chosen as the film manufacturing method because of its numerous benefits over solvent casting. Firstly, thicker films can be made for absorption experiments compared to the thin films typically generated by solvent casting Secondly, hot-melt pressing provides an improved capability to make uniform solid films. The solvent casting of films has been known to cause layering, with the added risk of solvent molecules remaining trapped in the films. Thirdly, hot-melt pressing is more time-efficient and is not limited by the time taken to evaporate solvent as is the case with solvent casting [42].

The films used in this study were made in two thicknesses, 0.1 mm for water diffusion and WAXS and 0.5 mm for water absorption and density measurements. The hot-melt pressing process involved the pressing of each material in a metal frame sandwiched between Kapton films, steel plates, and the hot plates of the press, Figure 2, at 170-260°C, depending on the material (see Paper 1 for more details). A pressure of 15 ± 0.5 t was applied for 5-7 min. The generated films were left to equilibrate to room temperature under weights of 8.9 ± 0.1 kg, after which they were cut into suitable shapes for the respective experiments. It was evident from the hot-melt pressing that M_n had a great impact with a high M_n being required to produce films that do not easily break when handled. For highly substituted

CAB, its M_n of 15 kDa was too low, making the material brittle and unable to form films during hot-melt pressing.

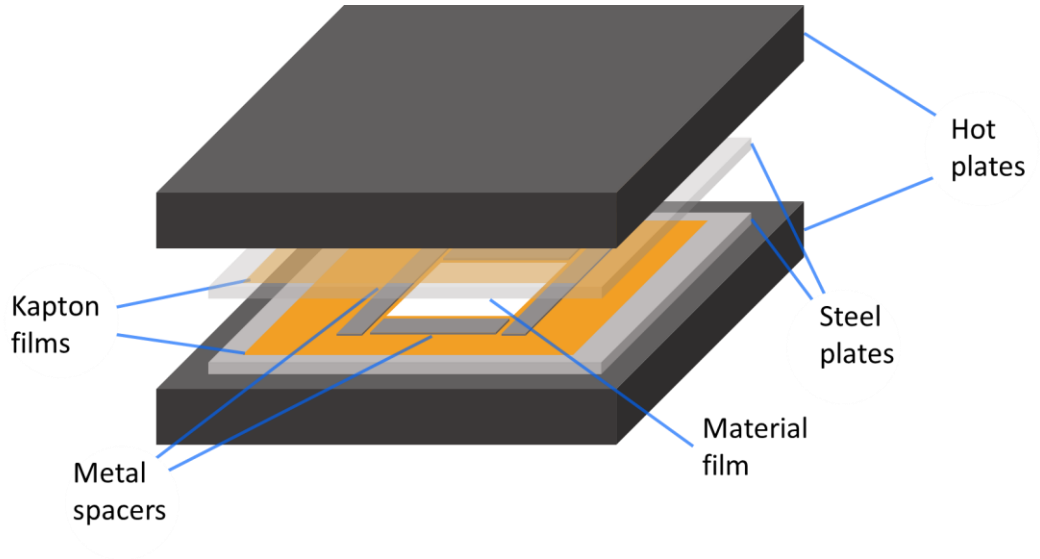

Figure 2. Illustration of the hot-melt pressing sandwich for film production.

6.3 Thermal Properties: TGA and DSC

An important factor to consider when performing hot-melt pressing is each material's T_d, which was determined by a thermogravimetric analysis (TGA). The TGA method involved heating the sample from 30°C to 500°C at a heating rate of 10°C min^{-1} with a nitrogen flow of 60 mL min^{-1}. The reported value of T_d corresponds to the intersection of the tangent of the baseline and tangent at the inversion point of the degradation curve, determined using STARe Evaluation Software (Mettler Toledo, Switzerland). Differential scanning calorimetry (DSC) scans, with a heating rate of 10°C min^{-1} from 25°C to 250°C, were used to determine the T_g and the T_m of the material using the same software. It should be noted that the reported data corresponds to the first heating curve. T_g was determined by the standard midpoint calculation in the STARe software. T_m is reported as the peak value of the melt peak, while the area of the melt peak was used to calculate the melting enthalpy, which could be used to determine the crystallinity.

6.4 Water Absorption and Water Diffusion

Water absorption studies were performed on 0.5 mm thick films of each material. The films were weighed and measured after drying in an oven for 24 h at 60°C. They were then submerged in deionized water for 72 h in a vessel with controlled, slow stirring at 25 rpm, Figure 3. Film weight and dimensions were measured at predefined times after removing excess water. This allowed the determination of both the water absorption and the density of the films.

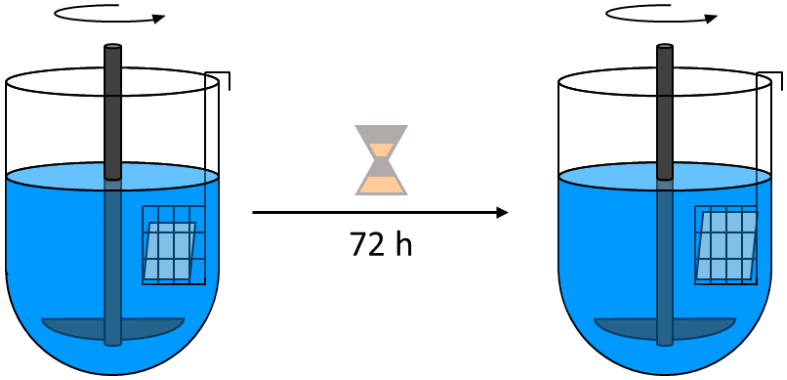

Figure 3. Illustration of the vessel with controlled stirring that was used for determination of water absorption. Note that the increase in the size of the films depicted in the figure is for visualization purposes only. In reality, the film swelling is not observable.

The water diffusion experiment was performed using a diffusion cell apparatus with tritium labeled water as a tracer, Figure 4. The sample films of the different materials were placed between the donor side and acceptor side of the diffusion cell apparatus, which were subsequently clamped together. Two corresponding 20 mL diffusion chambers, one on the donor side and one on the acceptor side, separated by a 0.1 mm thick sample film, were each filled with 15 mL water. A small amount of tritium water (T_2O) was added on the donor side, and the concentration on the acceptor side was monitored over time by measuring the radioactivity with a PerkinElmer Tri-Carb 2810 TR liquid scintillation analyzer.

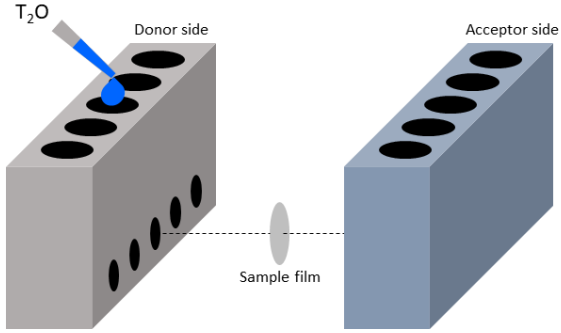

Figure 4. Illustration of the diffusion chambers where tritium water was added on the donor side and then passed through the sample film into the acceptor side.

From the change in radioactivity, the water permeability P (m^2 s^{-1}) of the sample film was calculated using Equation 2 [43]–[45],

$$\frac{2PA}{hV}t = -\ln\left(\frac{C_{d,0} - 2C_a(t)}{C_{d,0}}\right) \qquad (2)$$

where h (m) is the thickness of the film, V (m^3) is the total volume of the acceptor chamber, t (s) is the time, $C_{d,0}$ (mol m^{-3}) is the concentration on the donor side at time 0, and C_a (t) (mol m^{-3}) is the concentration on the acceptor side at time t. The permeation was calculated from the slope of the right side of Equation 2 over time. This equation is valid given the assumptions that the system is ideal, the chemical potential depends on concentration, no time-dependence on the concentration profile is present, the impact from stagnant layers at the film surface is negligible, and equal volumes on both the donor and acceptor side are present.

7 | Results and Discussion

This section addresses the characterization of the materials' chemical structure, HSP, and thermal properties. A section covering water absorption, water diffusion, and water vapor sorption isotherms are then presented, after which the effect of water absorption on density and microstructure are addressed. Finally, the HSP will be investigated as a potential tool for predicting performance based on the chemical structure of the cellulose esters.

7.1 Material and Film Properties

We have already established that the esters investigated are all highly modified when it comes to acyl groups, Table 1, and that the main difference between the esters is the length of the carbohydrate chain on the acyl (acetyl, propionyl, and butyryl). This does not seem to affect the T_d, Table 2, but it does have a great impact on T_g and T_m. CA has a T_g of 193ºC and when methylene groups are added to the side-chain, T_g decreases to 109ºC for CABIII. It is also worth noting that CAP is similar to CABII with respect to T_g, which indicates that butyrate has a larger impact than propionate. T_g is, as mentioned, an important factor as it depends on the strength of the attractive intermolecular forces between the chains in the material, with a higher T_g being indicative of stronger interaction forces. This, in turn, means that the increased side-chain length decreases the intermolecular forces, which could be associated with the side-chains pushing the polymer backbone further apart, creating weaker intermolecular interactions. Another aspect of the T_g is that it is similar for the starting material used as received (displayed as powder in the table) and for the hot-melt pressed films. The T_m, on the other hand, appears to be greatly influenced by the film-forming process. Only CA and CABI still have a detectable T_m after being melt processed, although unprocessed powders for all materials initially had detectable T_m. The T_m is related to the crystallinity of the material, thus implying that an increased side-chain length or average side-chain length on acyl above that of CABI results in amorphous films that show no T_m. Although CA and CABI do exhibit T_m, the area under the curve, which is directly related to the enthalpy of formation, shows a significant difference from powder to film. This was investigated further to show the significance of processing history. The next section addresses how these materials, and their different thermal properties affect their interactions with water.

Table 2. Thermal properties of the esters and EC showed as T_d, T_g, T_m, and the enthalpy of fusion (ΔH_f). T_d is only for powder.

Material	T_d [ºC]	T_g [ºC]		T_m [ºC]		ΔH_f [J g^{-1}]	
		film	powder	film	powder	film	powder
CA	355	193	191	230	233	1.00	7.74
CAP	356	143	140	-	201	-	4.14
CABI	365	154	155	238	241	6	10.64
CABII	356	136	137	-	168	-	11.17
CABIII	353	109	100	-	143	-	12.30
EC	338	126	121	177	174	4.35	6.40

7.2 Water Absorption, Diffusion, and Sorption Isotherms

The materials used in this study are relatively water-resistant, which is evident from the water absorption and water sorption data in Figure 5, however, CA tends to absorb more water and has a higher water diffusion compared to the other materials. Note that the order presented along the x-axis corresponds to the order of increasing side-chain length and an increasing DS of butyrate in the case of CAB. The cellulose ether, EC, is presented at the end. It can be observed that the water absorption decreases with an increased side-chain length from CA to CABIII. It appears, similarly to the T_g, that CAP water absorption behavior falls somewhere between CABI and CABII. In terms of the water diffusion rate, although a similar observation can be made, it is notable that both CAP and CABII

display a lower rate of water diffusion than CABIII, which is unexpected. The reason for this could be debated but a potential reason is that small cracks may have been formed in the CABIII films during hot-melt pressing or diffusion experiments. This is based on the difficulty experienced during CABIII film formation, when crack formation made the production of intact films challenging. The film integrity is more critical for diffusion experiments than absorption because the latter only depends on a weight increase. For comparison, EC seems to absorb and diffuse water similarly to CABI.

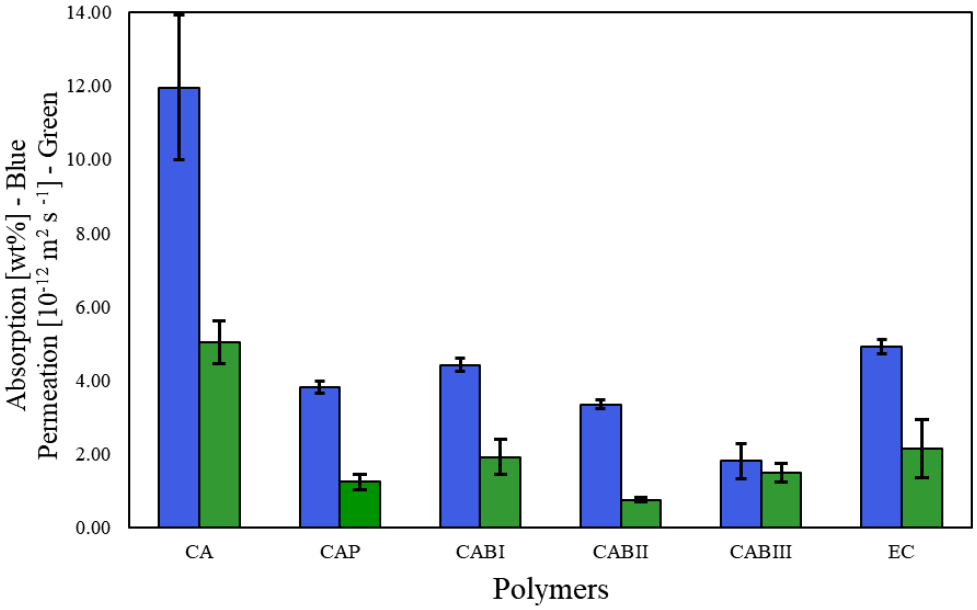

Figure 5. Water absorption (blue) and water diffusion (green) for CA, CAP, CABI, CABII, CABIII, and EC with standard deviation.

Water absorption and diffusion measurements were conducted on fully wetted films, which are important for packaging materials. Yet another interesting feature is how different humidity can affect the materials. It is evident, in Figure 6a, that CA and EC show a hysteresis effect, meaning that, at a certain point during absorption, they start to demonstrate an increased absorption per humidity step compared to similar steps going down again during desorption. This sudden increase in the amount of water absorbed was shown for EC, despite its relatively low amount of absorbed water. Interestingly, CABI absorbs a similar amount of water but does not show any hysteresis. This indicates that the molecular structure affects the water absorption process. These structural effects could manifest in the process of swelling. Compared to EC, CA shows a much larger hysteresis but also absorbs more water, *i.e.*, it requires more water to be absorbed into the structure to get an effect in the structure. This is further demonstrated in Figure 6b, where EC is depicted as requiring few water molecules per monomer to begin deforming. For CA, the point at which deformation/swelling begins is at 60% RH. In the literature, the presence of a hysteresis effect has been linked to the deformation of the polymer matrix [46]. This deformation could allow more water to enter and create clusters. In keeping with this explanation, it can be concluded that since CA and EC both exhibit hysteresis they might also show an extent of clustering that other esters with longer side-chains exhibit less of.

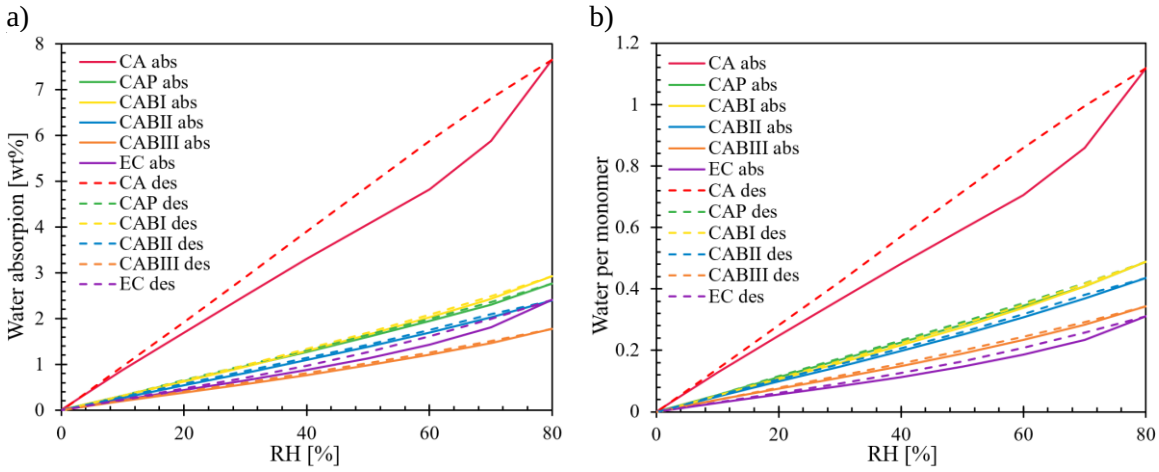

Figure 6. Water sorption curves for the esters and EC where a) is water absorption in wt% and b) is the number of water molecules per monomer at RH ranging from 0 to 80%.

To support this statement regarding clustering, MD simulations were performed on CA and CAP at two different RHs, *i.e.*, 40% and 80% RH. Figure 7, from Paper II, shows the results of the simulations, where the probability of larger clusters increases for CA when the humidity increases from 40 to 80% RH. The probability of finding one or two water molecules close to each other is, therefore, larger at 40% RH than 80% RH, while the probability of larger clusters is greater at 80% RH. CAP also shows a less pronounced effect of the RH but a tendency of an increase in the probability of larger water clusters at higher RH. Furthermore, CA has a higher probability of forming larger water clusters compared to CAP at the same RH. If this is compared to the sorption data, it can be concluded that CA has a higher probability to form larger clusters than CAP, which could support the existence of hysteresis for CA and the lack of it for CAP.

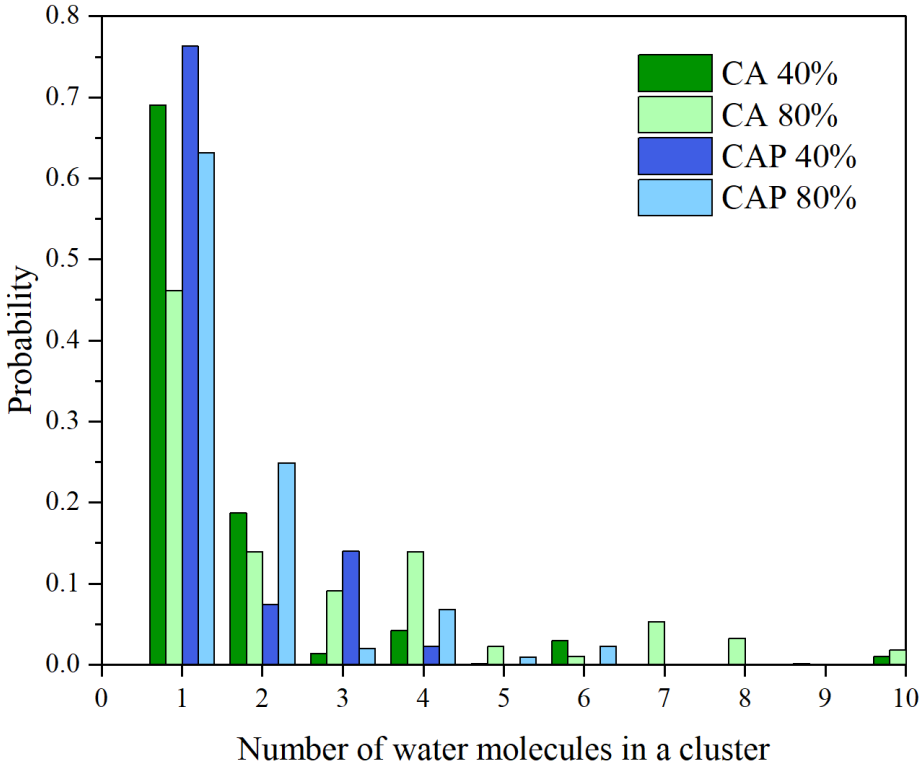

Figure 7. Clustering probability for different cluster sizes for CA and CAP at 40 and 80% RH, respectively.

7.3 Effect of Water Absorption

So far, water absorption and diffusion have been discussed. The sorption isotherms and simulations show that water interacts more strongly with CA, allowing the formation of water clusters. However, this does not directly imply that CA is structurally affected, while its closest ester, CAP, is not. By studying the volume change and, therefore, the density and absorption, one can infer more about structural changes. The density for hot-melt pressed films was measured in dry and wetted states, Figure 8, from which two observations were made. Firstly, the density decreases for the esters with increased side-chain length, which is evident for CABI to CABIII. The longer side-chains increase the distance between the polymer backbones, resulting in an expected decrease in the density. The second observation, which was not expected, was that the density appears to be higher for all materials in the wetted state than in the dry state. A similar increase was observed in the simulations of CA and CAP, see Table 4 in Paper II. This increase in densities indicates that the materials do not swell. If a material swells, the volume increase occurring when water, with a density of 1 g cm^{-3}, enters the system, would result in the density decreasing towards that of water. Instead, the measured increase in density in these results means that, unlike when a material swells, the water primarily enters empty voids of the polymer films and/or the water causes a reorientation of the structure upon entry, which enables closer packing of the chains. Nevertheless, the fact that all the materials had a higher density when wet does not explain why CA and EC showed hysteresis. A closer look into the microstructure was performed to investigate if structural changes occurred.

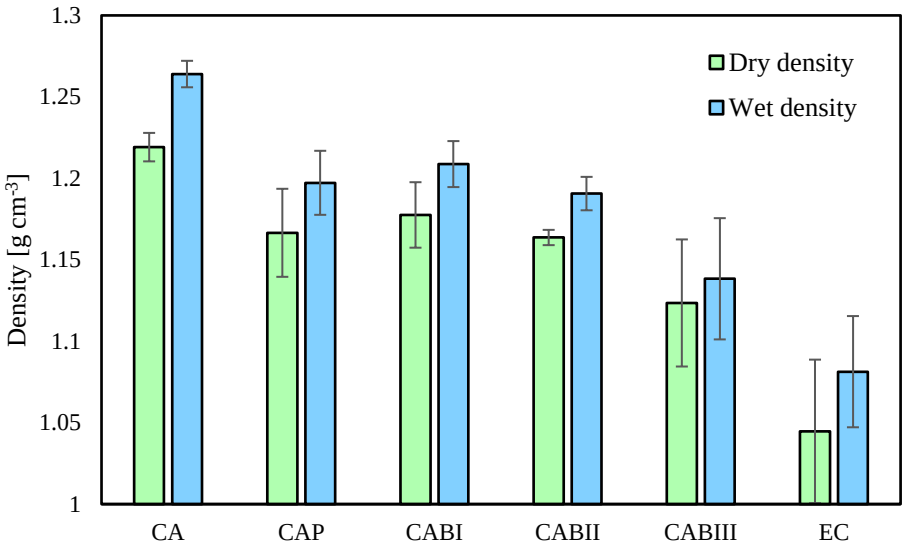

Figure 8. Density for wetted (blue right) and dried films (green left) of CA, CAP, CABI, CABII, CABIII, and EC.

WAXS is commonly performed to determine a value for crystallinity, however, in this study, the crystallinity has not been calculated. Instead, the focus was on the diffraction patterns. Figure 9 shows WAXS curves on dry and wet films of each material. All materials show a similar overall curve with two wide signals, centered around 0.5 $Å^{-1}$ and a slightly lower and broader signal at 1.5 $Å^{-1}$. By comparing dry films, the signals change from uneven ones, CA to CABI, with many smaller peaks to smoother, stronger curves with two peaks for CABII to CABIII. CAP is similar to CABII and CABIII. As the spectrum represents different plane distances, the multiple peaks in CA and CABI mean that they have many distinct packing patterns, while broad smooth signals like those of CAP, CABII, and CABIII mean more random orientations, which can be regarded as amorphous. At the same time, the intensity difference between signal peaks compared to the valley increases from CABI to CABIII, indicating that longer side-chains favor a microstructure with two different packing distances. When it comes to water absorption, CA has a peak that decreases at 1.3 $Å^{-1}$ and broadens at 1.6 $Å^{-1}$. The latter was observed for CABI as well, while the other materials only have a slight peak shift, with the lowest shift for CABIII. The decrease in the shift for the wetted samples from CA to CABIII corresponds to their decreased water absorption discussed in the previous section. This peak shift could be interpreted as a decrease in planar distances, indicating a denser microstructure, supporting the measured increase in density upon water absorption.

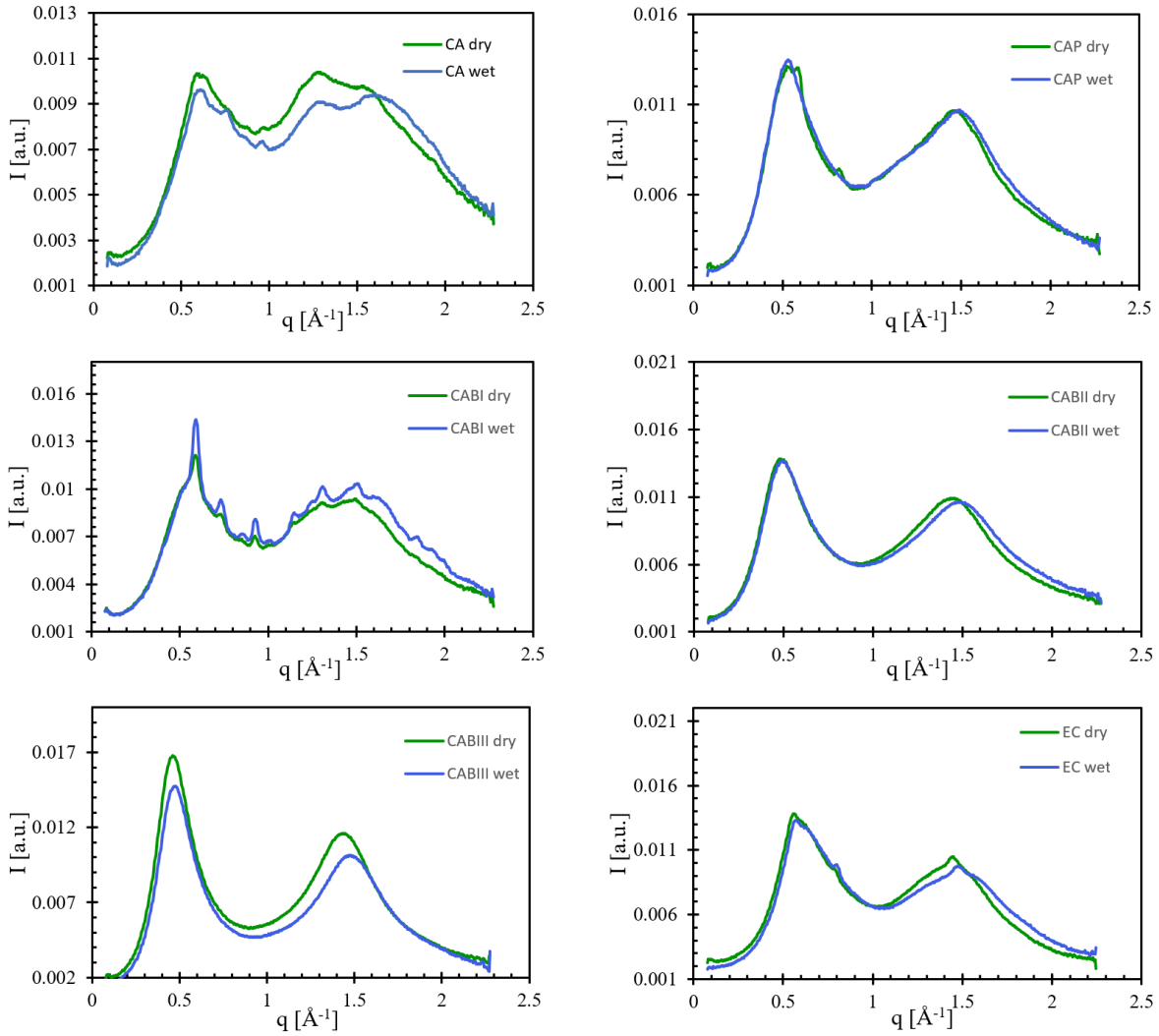

Figure 9. WAXS curves for dry and wet films of CA, CAP, CABI, CABII, CABIII, and EC. The figure has been modified from Nilsson et al. [48].

7.4 HSP as a Prediction Tool

Thus far, we have investigated how properties like T_g, water absorption, and microstructure change for the different materials as well as how water can change the microstructure. Can the observed properties be predicted by knowing the chemical structure of the materials? To investigate this, the materials' HSP values and their relations to the different properties will be discussed below. Note that the HSP were analyzed from the perspective of interaction energies rather than solubility.

As mentioned above, the hydroxyl groups have been used previously as an indicator for water sensitivity but also for other properties like T_g [47]. This is extensively discussed in Paper I and II but, to summarize, Paper I concluded that the hydroxyl groups of the materials did not show any apparent relation to the properties of the materials and Paper II concluded that water does not coordinate with the existing hydroxyl groups. This contradicts previous CAP and EC studies, where an increase in hydroxyl groups correlates to both T_g and water absorption [18], [45].

Figure 10 shows the three HSP for the materials plotted against their T_g. Overall, an increase in either of the three HSP increases the T_g, which is expected since they all represent the strength of different intermolecular interactions and are directly linked to properties like the T_g. Of all the HSP, the polar forces appear to be more linearly related, which is in agreement with the fact that water interacts with itself mainly via polar and hydrogen bonding forces. Note that EC does not follow the trend observed

for the esters, meaning that the correlation observed for the esters cannot be directly transferred to ethers like EC. For the other parameters, dispersion, hydrogen, and total HSP, EC follows closer to the trend observed for the esters. A conclusion from these graphs is that the increase in side-chain length decreases all HSP parameters in a similar order as the T_g and that there is a large difference between acetyl (CA) and the low modified butyryl (CABI). The addition of a few butyryl groups (DS 0.71) changes the properties significantly, suggesting a critical value of average chain length. By looking at the difference between CABI, CABII, and CABIII, one could assume a similar difference for CAP if three different DS were available. A CAP with low DS might be closer to CA in HSP and thus close the gap observed in the data, but this is only speculative at this stage and would warrant further study.

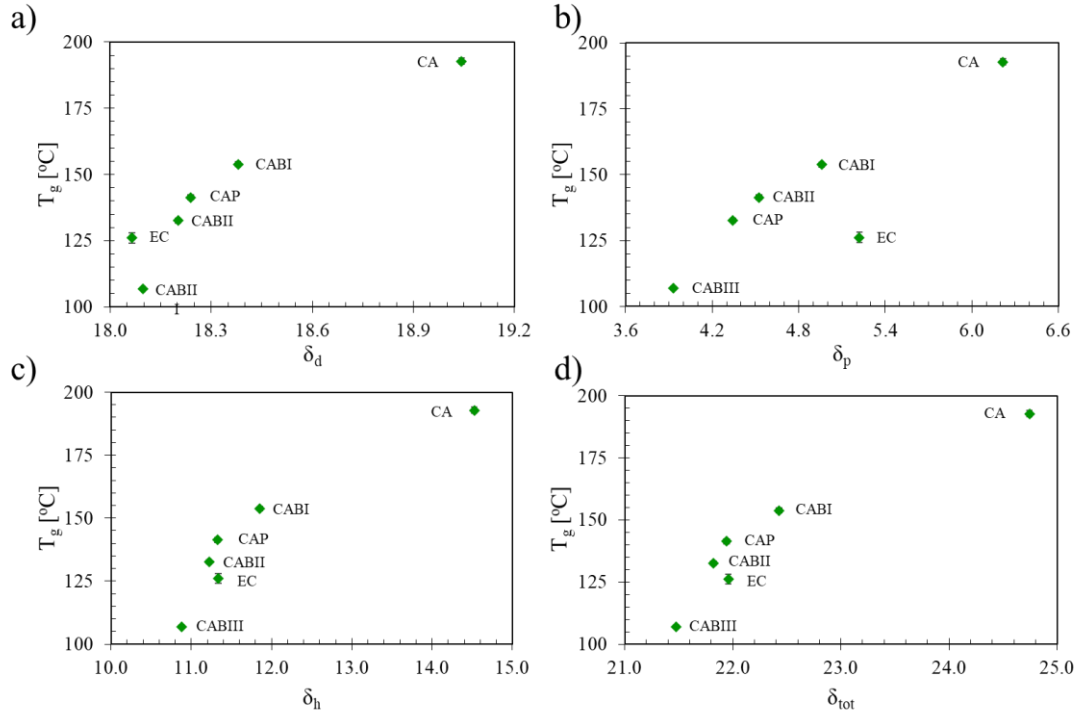

Figure 10. T_g for the different materials plotted against the different HSP δ_d, δ_p, δ_h, and δ_{tot}. The figure has been modified from Nilsson et al. [48].

There is a trend between all the HSP and T_g, with an exponential decrease in T_g occurring the more extended the side-chains get. There is also a general trend of decreasing water permeation and absorption when the HSPs decrease, see Figure 11. Comparably, the polar parameter, δ_p, maintains a reasonably linear trend when EC is included, whereas δ_d shows EC as an outlier. The similarity between δ_h and δ_{tot}, Figure 11c and 11d, means that the total HSP depends more on the hydrogen parameter than the others. Therefore, for the materials studied, it is important to note that the total parameter is not suitable since the polar parameter shows a better correlation to the T_g for the esters. The conclusion from this section is that it is not necessarily enough to exclusively study the total HSP. Instead, one needs to examine the building blocks of the total HSP, namely the different interaction parameters, to determine exactly what effect small changes in the chemical structure could have on the interaction energies of the material.

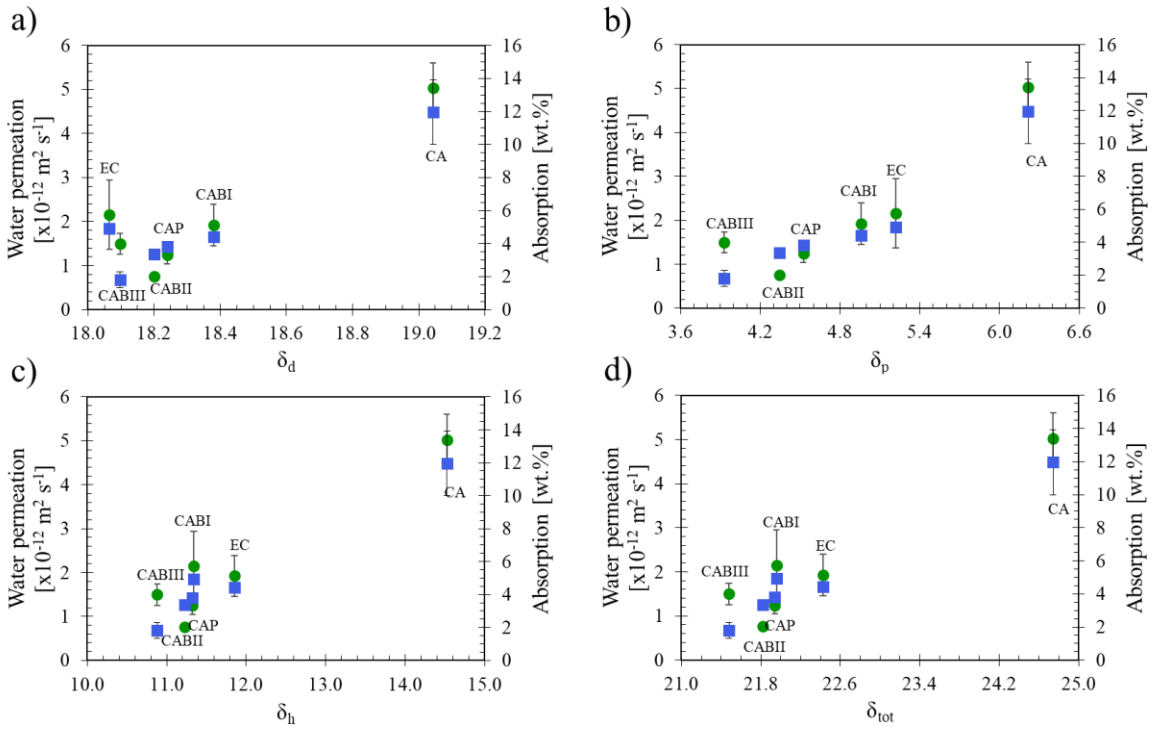

Figure 11. Water permeation and water diffusion plotted against the different HSP δ_d, δ_p, δ_h, and δ_{tot}. The figure has been modified from Nilsson et al. [48].

This leads to the following question: is the HSP able to predict that, of the esters, only CA would show a hysteresis effect? To investigate this, the area between the absorption and desorption curves in Figure 6 were plotted against the polar parameter, which was shown to have the most linear relation for water absorption, see Figure 12. It is evident that any side-chain length longer than acetyl appears to remove the hysteresis and that a cellulose derivative, at least for a cellulose ester, needs a polar parameter below five to remove the hysteresis and any subsequent deformation caused by excess absorbed water. For reference, water has a polar parameter of 16 [38], which means that materials with a polar parameter relatively far from water start to be significantly affected. The attraction is then high enough for water to be absorbed in the structure and affect the structure when the polar parameter gets within range.

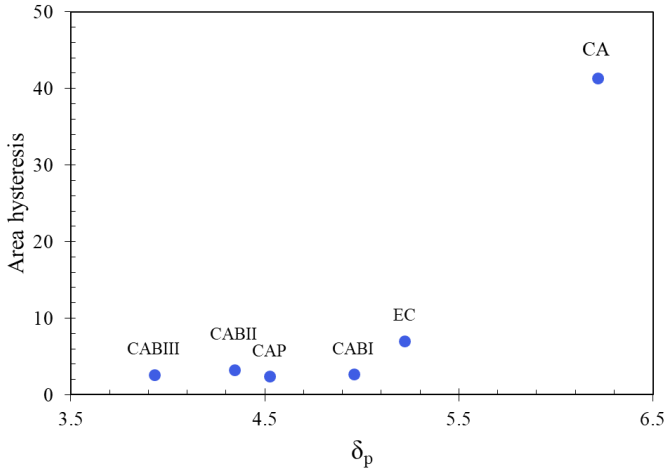

Figure 12. Area of the sorption hysteresis for all materials as a function of their δ_p.

We have now investigated the different components of the HSP but, by separating the molar volume from the HSP, one could go one step further and look into the energies. According to Equation 1, the

HSP consist of intermolecular energies divided by the molar volume. Thus, the different energies for dispersion, polar, and hydrogen bonding are plotted against molar volume (V_{molar}) in Figure 13. For the esters, the dispersion energy increases when the side-chain length increases from CA to CABIII, which is directly related to the fact that the extra carbohydrates on the side-chains only interact via dispersion forces. The opposite trend is observed for polar forces and to a lesser extent for hydrogen forces, despite only the addition of the dispersion forces. By plotting T_g and water absorption against V_{molar}, a strong correlation is seen for the esters. As discussed previously, T_g strongly depends on the intermolecular interactions. Therefore, when adding groups with dispersion forces, the total energy of the material should increase as side-chain length increases. Instead, these properties decreased with increased side-chain length because the effect of extra methylene groups adding more volume to the molecular structure is greater than that of the increased dispersion forces. This decrease in thermal and absorption properties is significant since, as the molar volume increases, the short distance and strong interactions, like hydrogen bonding, will be screened out by the increased distance between hydrogen bonding groups.

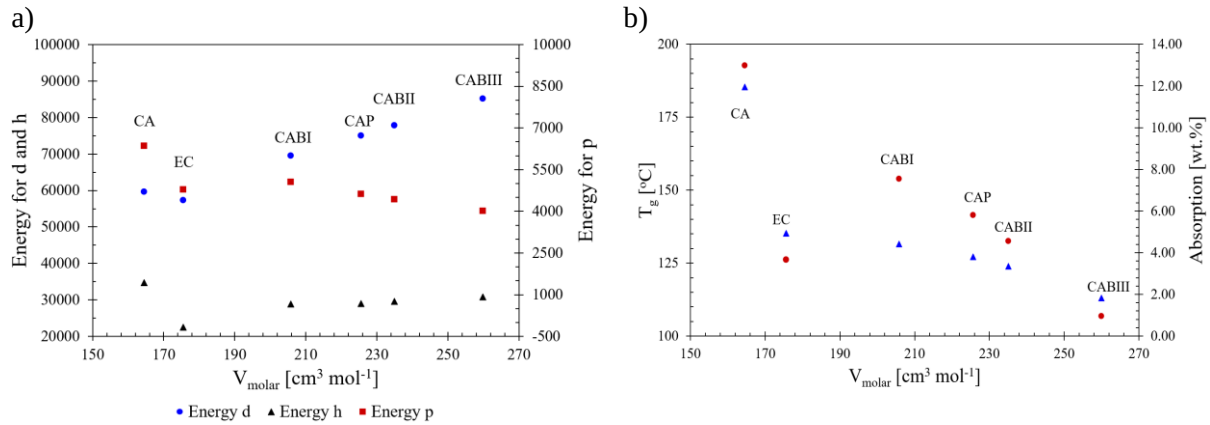

Figure 13. a) Energy for dispersion, hydrogen, and polar interactions against molar volume. B) T_g and water absorption against molar volume of the different materials. The figure has been modified from Nilsson et al. [48].

8 | Conclusion and Future Perspective

Increasing the side-chain length of CA by one or two methyl groups (CAP and CAB, respectively) significantly decreases T_g, water absorption, and water diffusion. This is shown, via dissection of the HSP, to be related to an increase in molar volume. An increase in molar volume results in a screening effect of hydrogen bonding, meaning that the distances between hydrogen interacting groups increase to such a degree that they cannot interact to the same extent as before the screening.

CA is shown to be more affected by water than the other esters, with an increase in side-chain length having a significant effect on water interaction, making the material less prone to have structural changes due to water.

The HSP are shown to correlate more for some properties than others. The dispersion forces relate linearly to T_g for all derivatives, while the polar parameter is more suitable for the esters. Water absorption is more related to the polar parameter than the other parameters. To use HSP as a more general tool for prediction, one needs to know more about how different substituents affect different properties like thermal properties and water absorption. To determine this, an expanded scope of polymers needs to be investigated beyond the esters with increasing side-chain lengths studied in this thesis.

The continuation of this work has two tracks. One is a deeper investigation of water sorption kinetics of the different cellulose esters. This will be done by conducting dynamic vapor sorption experiments and dynamic mechanical analysis at different humidity. The second track involves the construction and validation of a permeation instrument and its subsequent application to investigate the influence of RH on oxygen permeation.

9 | Acknowledgements

The financial support from FORMAS is gratefully acknowledged.

I would like to express my gratitude to the following people, who have supported me and without whom this thesis would not exist:

Professor Anette Larsson, my main supervisor, for her wisdom, positiveness, late-night emails, and excellent guidance, which have made me into the scientist I am today.

Professor Gunnar Westman and Professor Christian Müller as co-supervisors, for their support and guidance, when I needed it.

My co-authors for Paper I and Paper II are acknowledged for all their contribution.

My reference group in Vinnova competence center FibRe for all the feedback on my work.

Treesearch, which has provided me with a necessary scientific network and collaboration opportunities.

My girlfriend, Louise Samuelsson, who has supported me throughout my work.

Ms. Roujin Ghaffari, for all the support and friendship by being my go-to colleague.

All my office mates and colleagues with whom I have and will continue to create memories.

Ms. Rydvikha Govender for providing an excellent linguistic review of this thesis.

Last, but not least, my family and friends who have inspired me and formed me into the person I am today.

10 | References

[1] Plastic Europe - Association of Plastics Manufactures, “Plastics – the Facts 2020,” *Plast. Eur.*, pp. 1–64, 2020.

[2] Statistisk årsbok för Sverige, Statistical yearbook of Sweden, 2011, Statistics Sweden, Communication, Department Box 24300, SE-104 51 Stockholm, ISSN 1654-4420

[3] J. A. Enderby, “Water absorption by polymers,” *Trans. Faraday Soc.*, vol. 51, no. 106, pp. 106–116, 1955, doi: 10.1039/tf9555100106.

[4] S. Gårdebjer, M. Andersson, J. Engström, P. Restorp, M. Persson, and A. Larsson, “Using Hansen solubility parameters to predict the dispersion of nano-particles in polymeric films,” *Polym. Chem.*, vol. 7, no. 9, pp. 1756–1764, 2016, doi: 10.1039/c5py01935d.

[5] Y. Ran, F. Byrne, I. D. V. Ingram, and M. North, “Resin Swelling in Mixed Solvents Analysed using Hansen Solubility Parameter Space,” *Chem. - A Eur. J.*, vol. 25, no. 19, pp. 4951–4964, 2019, doi: 10.1002/chem.201900228.

[6] S. Ramanaiah, P. R. Rani, T. V. M. Sreekanth, and K. S. Reddy, “Determination of Hansen Solubility Parameters for the Solid Surface of Cellulose Acetate Butyrate by Inverse Gas Chromatography,” *J. Macromol. Sci. Part B*, vol. 50, no. 3, pp. 551–562, 2011, doi: 10.1080/00222341003784527.

[7] S. Ramanaiah, P. Reddi Rani, and K. S. Reddy, “Hansen solubility parameters for the solid surface of cellulose acetate propionate by inverse gas chromatography,” *J. Macromol. Sci. Part B Phys.*, vol. 51, no. 11, pp. 2191–2200, 2012, doi: 10.1080/00222348.2012.669681.

[8] R. C. Ong, T. S. Chung, B. J. Helmer, and J. S. De Wit, “Novel cellulose esters for forward osmosis membranes,” *Ind. Eng. Chem. Res.*, vol. 51, no. 49, pp. 16135–16145, 2012, doi: 10.1021/ie302654h.

[9] K. Kamide, Cellulose and Cellulose Derivatives Molecular Characterization and its Applications, *Elsevier* 2005, ISBN: 0-444-82254-2.

[10] D. Klemm, B. Philipp, T. Heinze, U. Heinze, and W. Wagenknecht, *Comprehensive Cellulose Chemistry: Volume I: Fundamentals and analytical Methods*, vol. l. 1998.

[11] H. Ost-Hannover, “Geschichtliches über die Celluloseacetate,” *Zeitschrift für Angew. Chemie*, vol. 366, pp. 1304–1306, 1911.

[12] D. A. Eichengrün, “Bekanntes und Unbekanntes aus der Acetylcellulose-Industrie.” Chemiker-Zeitung, pp. 25–36, 1927.

[13] P. Rustemeyer, “History of CA and evolution of the markets,” *Macromol. Symp.*, vol. 208, pp. 1–6, 2004, doi: 10.1002/masy.200450401.

[14] A. J. Sayyed, N. A. Deshmukh, and D. V. Pinjari, “A critical review of manufacturing processes used in regenerated cellulosic fibres: viscose, cellulose acetate, cuprammonium, LiCl/DMAc, ionic liquids, and NMMO based lyocell,” *Cellulose*, vol. 26, no. 5, pp. 2913–2940, 2019, doi: 10.1007/s10570-019-02318-y.

[15] M. A. Boogard, D. A. Godfrey, T. J. Fredrick, “United States Statutory Invention Registration", Reg. No.: US H2083 H, Filed Mar 27, 2001, Published Oct. 7, 2003.

[16] J. V Koleske (ed), Paint and Coating Testing Manual - 15th edition of the Grdner-Sward Handbook, 1995, ASTM International, ISBN 978-0-8031-7017-9

[17] S. Zhang, R. Zhang, Y. C. Jean, D. R. Paul, and T. S. Chung, “Cellulose esters for forward osmosis: Characterization of water and salt transport properties and free volume,” *Polymer*, vol. 53, no. 13, pp. 2664–2672, 2012, doi: 10.1016/j.polymer.2012.04.024.

[18] R. C. Ong, T. S. Chung, B. J. Helmer, and J. S. De Wit, “Characteristics of water and salt transport, free volume and their relationship with the functional groups of novel cellulose esters,” *Polymer*, vol. 54, no. 17, pp. 4560–4569, 2013, doi: 10.1016/j.polymer.2013.06.043.

[19] A. Ibrahim and R. Ali, “Characterization of microparticles prepared by the solvent evaporation method, use of alcohol-soluble cellulose acetate butyrate as a carrier,” *J. Pharm. Pharmacogn. Res.*, vol. 8, no. 4, pp. 336–345, 2020.

[20] Cambridge Polymer Group Inc., “Glass Transition by DMA” CPGAN #035, Cambridge Polymer Group, Inc.(2014).

[21] U. T. Kreibch and H. Batzer, “Einfluß der Segmentstruktur und der Vernetzung auf den Glasübergang Tg. Möglichkeiten der Vorausberechnung von Tg über die Kohäsionsenergie Ecoh,” *Die Angew. Makromol. Chemie*, vol. 83, no. 1, pp. 57–112, 1979, doi: 10.1002/apmc.1979.050830105.

[22] Semicrystalline Polymers, Electron Microscopy of Polymers 295–327, Springer Berlin Heidelberg, 2008, doi:10.1007/978-3-540-36352-1_17.

[23] A. C. Puleo, D. R. Paul, and S. S. Kelley, “The effect of degree of acetylation on gas sorption and transport behavior in cellulose acetate,” *J. Memb. Sci.*, vol. 47, no. 3, pp. 301–332, 1989, doi: 10.1016/S0376-7388(00)83083-5.

[24] T. Danjo and T. Iwata, “Syntheses of cellulose branched ester derivatives and their properties and structure analyses,” *Polymer (Guildf).*, vol. 137, pp. 358–363, 2018, doi: 10.1016/j.polymer.2018.01.009.

[25] D. S. Reid and H. Levine, “Beyond Water Activity: Recent Advances Based on an Alternative Approach to the Assessment of Food Quality and Safety,” *Crit. Rev. Food Sci. Nutr.*, vol. 30, no. 2–3, pp. 115–360, 1991, doi: 10.1080/10408399109527543.

[26] D. Gabor (Naiaretti) and O. Tita, “Biopolymers Used in Food Packaging : a Review,” *Acta Univ. Cibiniensis Ser. E FOOD Technol.*, vol. XVI, no. 2, pp. 3–19, 2012.

[27] H. Deng, C. T. Reynolds, N. O. Cabrera, N. M. Barkoula, B. Alcock, and T. Peijs, “The water absorption behaviour of all-polypropylene composites and its effect on mechanical properties,” *Compos. Part B Eng.*, vol. 41, no. 4, pp. 268–275, 2010, doi: 10.1016/j.compositesb.2010.02.007.

[28] H. Hatakeyama and T. Hatakeyama, “Interaction between water and hydrophilic polymers,” *Thermochim. Acta*, vol. 308, no. 1–2, pp. 3–22, 1998, doi: 10.1016/s0040-6031(97)00325-0.

[29] J. Skalny and N. Hearn, “13 - Surface Area Measurements,” in *Handbook of Analytical Techniques in Concrete Science and Technology*, V. S. Ramachandran and J. J. Beaudoin, Eds. Norwich, NY: William Andrew Publishing, 2001, pp. 505–527.

[30] K. S. W. Sing, “Reporting physisorption data for gas/solid systems with special reference to the determination of surface area and porosity (Recommendations 1984),” *Pure Appl. Chem.*, vol. 57, no. 4, pp. 603–619, 1985, doi: doi:10.1351/pac198557040603.

[31] S. Rajabnezhad *et al.*, “Investigation of water vapour sorption mechanism of starch-based pharmaceutical excipients,” *Carbohydr. Polym.*, vol. 238, no. January, p. 116208, 2020, doi: 10.1016/j.carbpol.2020.116208.

[32] C. Driemeier, F. M. Mendes, and M. M. Oliveira, “Dynamic vapor sorption and thermoporometry to probe water in celluloses,” *Cellulose*, vol. 19, no. 4, pp. 1051–1063, 2012, doi: 10.1007/s10570-012-9727-z.

[33] I. del Gaudio, E. Hunter-Sellars, I. P. Parkin, D. Williams, S. Da Ros, and K. Curran, “Water sorption and diffusion in cellulose acetate: The effect of plasticisers,” *Carbohydr. Polym.*, vol.

267, no. January, p. 118185, 2021, doi: 10.1016/j.carbpol.2021.118185.

[34] M. Simon and R. Fulchiron, “Experimental and Modelling Studies of Water Sorption Properties of Cellulosic Derivative Fibers, Research Square, 2021, https://doi.org/10.21203/rs.3.rs-586610/v1

[35] S. Gårdebjer, M. Larsson, T. Gebäck, M. Skepö, and A. Larsson, “An overview of the transport of liquid molecules through structured polymer films, barriers and composites – Experiments correlated to structure-based simulations,” *Adv. Colloid Interface Sci.*, vol. 256, pp. 48–64, 2018, doi: 10.1016/j.cis.2018.05.004.

[36] J. Wang *et al.*, “A critical review of transport through osmotic membranes,” *J. Memb. Sci.*, vol. 454, pp. 516–537, 2014, doi: 10.1016/j.memsci.2013.12.034.

[37] A. Elidrissi, S. El barkany, H. Amhamdi, A. Maaroufi, and B. Hammouti, “New approach to predict the solubility of polymers application: Cellulose acetate at various DS, prepared from Alfa ‘Stipa -tenassicima’ of Eastern Morocco,” *J. Mater. Environ. Sci.*, vol. 3, no. 2, pp. 270–285, 2012.

[38] Hansen, C.M. (2007). Hansen Solubility Parameters: A User's Handbook, Second Edition (2nd ed.). CRC Press. https://doi.org/10.1201/9781420006834

[39] D. W. Van Krevelen and K. Te Nijenhuis, Cohesive Properties and Solubility, Properties of Polymers 4th edition, 2009, doi: B978-0-08-054819-7.00007-8

[40] G. Stiubianu, C. Racles, A. Nistor, M. Cazacu, and B. C. Simionescu, “Cellulose modification by crosslinking with siloxane diacids,” *Cellul. Chem. Technol.*, vol. 45, no. 3–4, pp. 157–162, 2011.

[41] W. G. Lee, D. Y. Kim, and S. W. Kang, “Porous Cellulose Acetate by Specific Solvents with Water Pressure Treatment for Applications to Separator and Membranes,” *Macromol. Res.*, vol. 26, no. 7, pp. 630–633, 2018, doi: 10.1007/s13233-018-6091-3.

[42] U. Siemann, *Solvent cast technology – a versatile tool for thin film production*. Progr Colloid Polym Sci, 130: 1–14, Springer-Verlag, 2005.

[43] B. Maciejewski, A. Ström, A. Larsson, and M. Sznitowska, “Soft gelatin films modified with cellulose acetate phthalate pseudolatex dispersion-structure and permeability,” *Polymers (Basel).*, vol. 10, no. 9, 2018, doi: 10.3390/polym10090981.

[44] G. Van den Mooter, C. Samyn, and R. Kinget, “Characterization of colon-specific azo polymers: A study of the swelling properties and the permeability of isolated polymer films,” *Int. J. Pharm.*, vol. 111, no. 2, pp. 127–136, 1994, doi: 10.1016/0378-5173(94)00102-2.

[45] J. Hjärtstam and T. Hjertberg, “Studies of the water permeability and mechanical properties of a film made of an ethyl cellulose-ethanol-water ternary mixture,” *J. Appl. Polym. Sci.*, vol. 74, no. 8, pp. 2056–2062, 1999, doi: 10.1002/(SICI)1097-4628(19991121)74:8<2056::AID-APP21>3.0.CO;2-Y.

[46] S. Okubayashi, U. J. Griesser, and T. Bechtold, “A kinetic study of moisture sorption and desorption on lyocell fibers,” *Carbohydr. Polym.*, vol. 58, no. 3, pp. 293–299, 2004, doi: 10.1016/j.carbpol.2004.07.004.

[47] J. Hjärtstam and T. Hjertberg, “Effect of Hydroxyl Group Content in Ethyl Cellulose on Permeability in Free Films and Coated Membranes,” *J. Appl. Polym. Sci.*, vol. 72, no. 4, pp. 529–535, 1999, doi: 10.1002/(sici)1097-4628(19990425)72:4<529::aid-app9>3.3.co;2-w.

[48] R. Nilsson, M. Olsson, G. Westman, A. Matic, and A. Larsson, “Screening of hydrogen bonds in modified cellulose acetates with alkyl chain substitutions,” *Carbohydr. Polym.*, vol. 285, no. November 2021, p. 119188, 2022, doi: 10.1016/j.carbpol.2022.119188.